

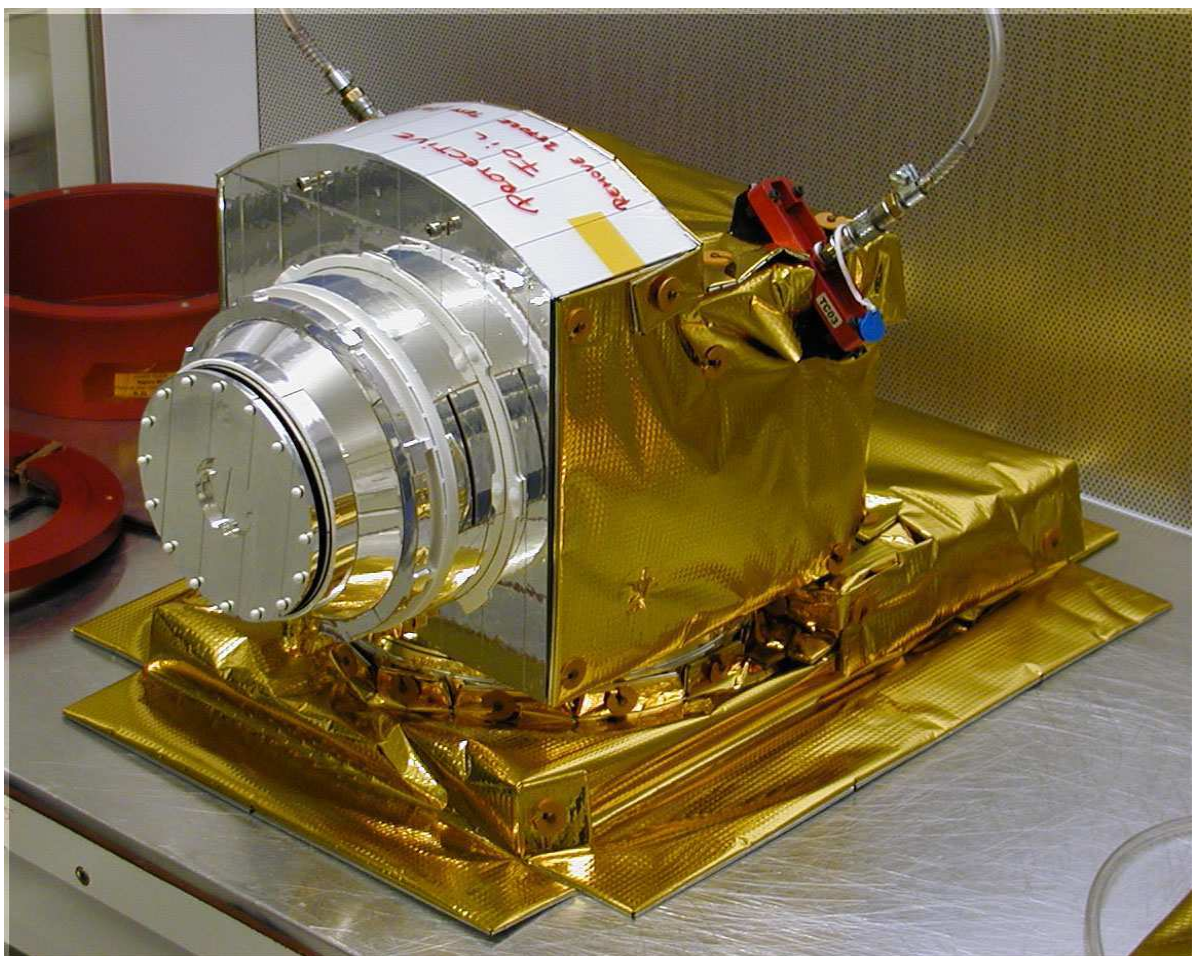
Venus Express

ASPERA-4

ELS Data Analysis Summary

v2.0

February 09, 2009



Neville Shane, Dhiren Kataria, Andrew Coates

Mullard Space Science Laboratory, University College London, UK

1. ASPERA-4 Electron Spectrometer

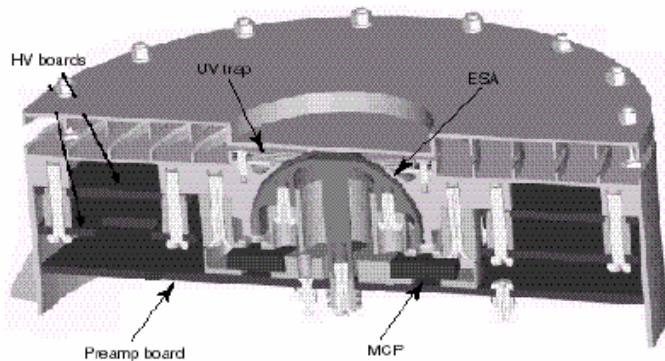


Figure 1: Cutaway diagram of ELS

the inner spherical electron deflection plate. The electrons hit a micro channel plate (MCP) after being filtered in energy by the analyzer plates. The plates are stepped in voltage to achieve an energy spectrum. Electrons with energies up to 20 keV/q will be measured, with a maximum time resolution of one energy sweep per four seconds. There are 16 anodes behind the MCP, each anode defining a 22.5 ° sector and each connected to a preamplifier. The ELS sensor will be mounted on the ASPERA-4 scan platform, on top of the NPI sensor, in such a way that the full 4- π angular distribution of electrons will be measured during each platform scan.

2. MSSL calibration facility

The design of MSSL's calibration facility for electron instruments is based on Marshall et al, 1986. The calibration system is housed in a cylindrical stainless steel vacuum chamber. A grounded μ -metal shroud inside the chamber, enclosed at both ends, ensures that the residual magnetic field inside the chamber is less than one tenth of the Earth's magnetic field; this results in an electron beam divergence of less than 1° at 1keV.

Light from a mercury UV lamp outside the vacuum chamber is transmitted through a quartz window on to a gold-coated quartz disc inside the chamber. Over 90% of the output wavelength of the lamp is at the 253.7nm mercury line. The energy of the incident UV light is just sufficient to knock photoelectrons out of the gold layer on the quartz disc and as a result, the kinetic energy of the ejected photoelectrons is small (~0.3eV). These electrons are then accelerated by an electric field and emerge through the grid with an energy defined by the applied voltage (between 5eV and 10keV). The intensity of the beam can be varied by placing one of a series of neutral density filters in front of the UV lamp. The cross-section of the resulting electron beam is approximately 120mm in diameter.

The instrument to be calibrated is mounted on a 2-axis rotary table, which allows movement of the instrument over the complete azimuthal and elevation

The ELS instrument was manufactured by South-west Research Institute (SwRI) in San Antonio, Texas as the Flight Spare for Mars Express. It represents a new generation of ultra-light, low-power, electron sensor (Barabash et al, 2004). It is formed by a spherical top-hat electrostatic analyzer and a collimator system (Figure 1). Particles enter the aperture at any angle in the plane of incidence.

Electrons are then deflected into the spectrometer by applying a positive voltage to



Figure 3: The Venus Express ASPERA-4 ELS sensor mounted in the MSSL calibration facility

angle response range. The mounting is such that the centre of the instrument aperture is at the centre of rotation of both the axes. This ensures that the centre of the aperture is always illuminated by the same area of the beam. A channeltron is mounted as close as possible to the instrument aperture in order to provide a constant reference to the beam intensity. A schematic diagram of the calibration facility is shown in Figure 2. A photograph of the Venus Express ASPERA-4 instrument inside the MSSL calibration facility is presented in Figure 3.

3. Energy-angle scans

All of the analyser parameters are extracted from the Energy (sweep voltage) – Angle scans carried out at the centre of each anode for beam energies of 10eV, 30 eV, 50eV, 70eV, 100eV, 200eV, 1 keV, 3 keV, 6 keV, 10 keV, 12 keV. An example plot at 200 eV is shown in Figure 4.

4. K-factors

Figure 5 is a plot of the lab-measured k-factor for the 10 energies, shown as different colour lines. Table 1 shows the energy-averaged k-factors for each anode.

Table 1: Energy sensitivity for each anode (eV/V)

0	1	2	3	4	5	6	7	8	9	10	11	12	13	14	15
10.490	10.627	10.824	10.956	11.077	11.192	11.310	11.397	11.315	11.193	11.007	10.808	10.558	10.419	10.355	10.363

A 4D polynomial fit to the values above gives the following relationship between k-factor (k) and anode (a):

$$(1) \quad k = 10.518 + 0.0424a + 0.0573a^2 - 0.00889 a^3 + 0.000323 a^4$$

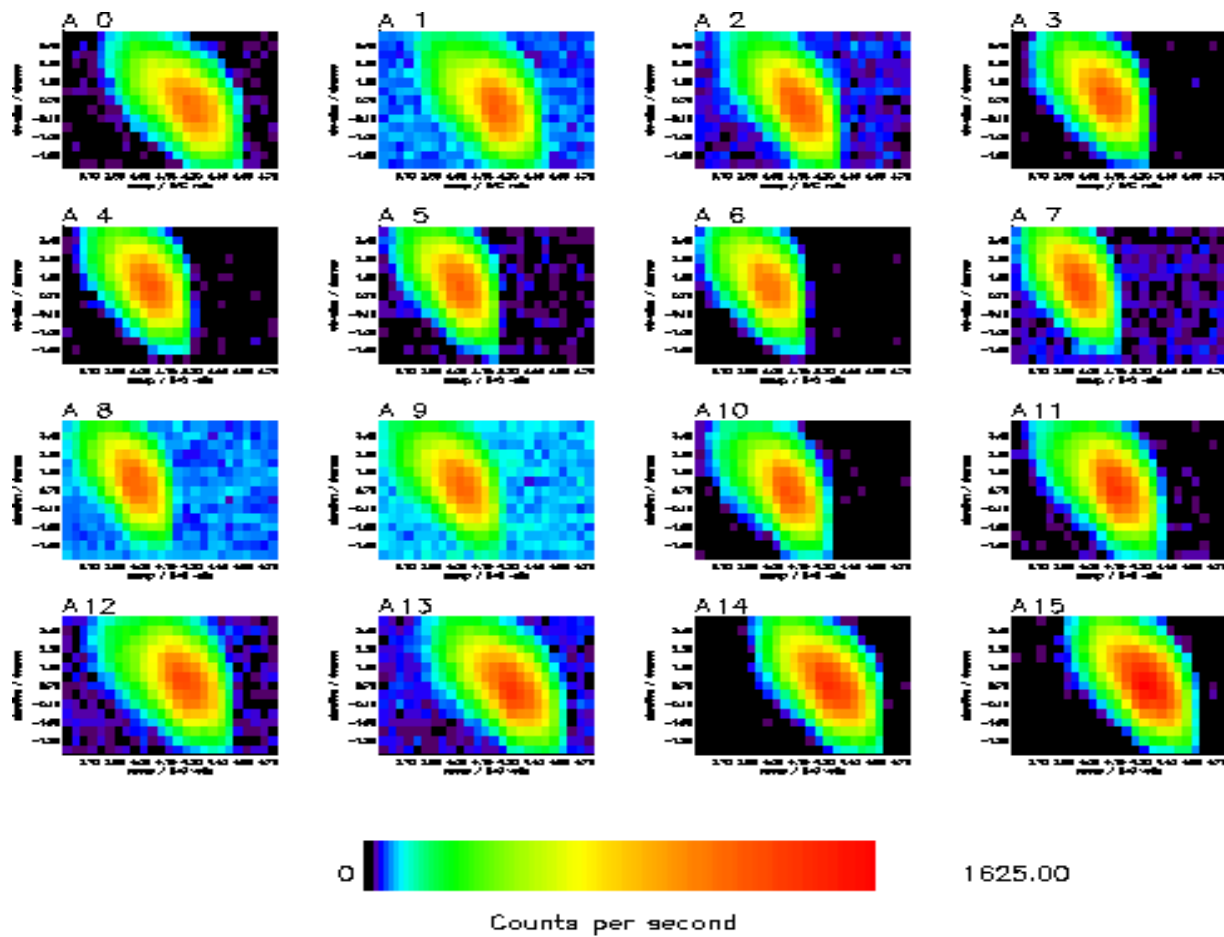


Figure 4: Energy-angle response of ELS at 200eV electron beam energy

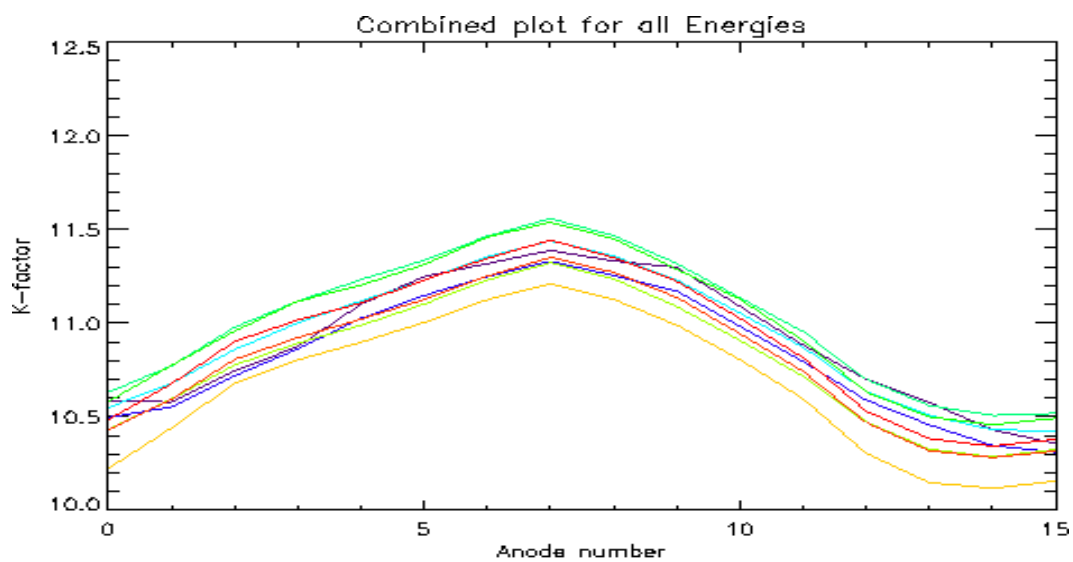


Figure 5: Plot of analyser k-factor across the 16 anodes for 10 beam energies

5. Energy Resolution

Figure 6 is a plot of the energy resolution across the 16 anodes. The measured values are given in Table 2.

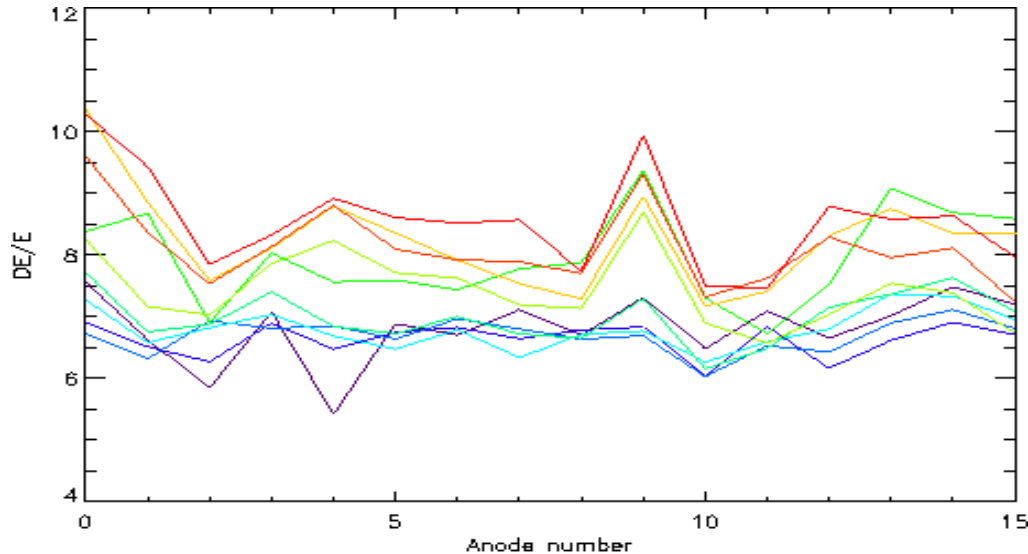


Figure 6: Plot of energy resolution across the 16 anodes for 10 beam energies

Table 2: Laboratory measured energy resolutions

Energy(eV) Anode	29.9200	50.3000	70.2000	100.400	199.990	970.000	3021.00	5994.00	9990.00	11997.0
0	7.56060	6.90909	6.72312	7.27587	7.72092	8.50001	8.24999	10.3585	9.60001	10.2789
1	6.63077	6.51376	6.31894	6.58139	6.75295	8.47059	7.16505	8.85577	8.36232	9.43137
2	5.84375	6.27102	6.93560	6.82143	6.87952	6.90908	7.03000	7.58824	7.53731	7.84849
3	7.07937	6.89624	6.81164	7.03614	7.40244	8.31249	7.85859	8.11000	8.13636	8.32654
4	5.41935	6.47620	6.85121	6.68675	6.84146	7.53125	8.23470	8.78788	8.80303	8.91752
5	6.88524	6.74758	6.63986	6.47561	6.72839	7.43750	7.71134	8.35714	8.09231	8.60825
6	6.70492	6.82524	6.96503	6.78750	7.00000	7.71875	7.62500	7.91752	7.92188	8.51579
7	7.11667	6.64357	6.80357	6.33751	6.72151	7.29032	7.18750	7.53609	7.89063	8.56842
8	6.70492	6.78431	6.63604	6.71606	6.65000	7.43750	7.13541	7.28866	7.70313	7.73958
9	7.31147	6.83496	6.69231	6.76830	7.29630	7.84376	8.69388	8.94950	9.30769	9.93815
10	6.48387	6.02885	6.03114	6.26507	6.15854	7.43750	6.89898	7.17000	7.31819	7.50000
11	7.09523	6.83962	6.52881	6.59524	6.48810	6.36364	6.57426	7.41176	7.62686	7.46000
12	6.65626	6.16667	6.42857	6.80233	7.15116	8.02941	7.03847	8.31429	8.28986	8.78640
13	7.01538	6.61817	6.89903	7.36781	7.36781	8.64707	7.54286	8.74528	7.95715	8.57693
14	7.48485	6.90991	7.11290	7.32955	7.63219	8.88235	7.38095	8.35515	8.11428	8.63460
15	7.19697	6.71171	6.81108	6.95454	7.08045	7.79412	6.73333	8.33962	7.24286	7.97116

Using the data in Table 2, we find that the energy resolution, $\Delta E/E$, for each anode can be fit to the log of the energy (E) by the equation:

$$(2) \quad \Delta E/E = m_0 + m_1 \log_{10}(E)$$

The coefficients m_0 and m_1 are given for each anode in Table 3:

Table 3: Coefficients for energy resolution straight line fit

Anode	0	1	2	3	4	5	6	7	8	9	10	11	12	13	14	15
m₀	4.969	4.749	5.507	6.063	4.293	5.366	5.780	5.735	5.991	4.928	5.302	6.190	5.141	5.943	6.469	6.347
m₁	1.211	0.998	0.528	0.555	1.143	0.724	0.585	0.533	0.394	1.098	0.516	0.256	0.805	0.626	0.475	0.339

6. Fine polar scans

The energy-angle scans also provide the peak response of the instrument for each energy. In order to obtain the relative response of the instrument, a fine scan is carried out at polar steps of 0.25 degrees across the polar range of $\pm 168.75^{\circ}$ at the peak elevation and voltage. Figure 7 is an example of the response at 100 eV.

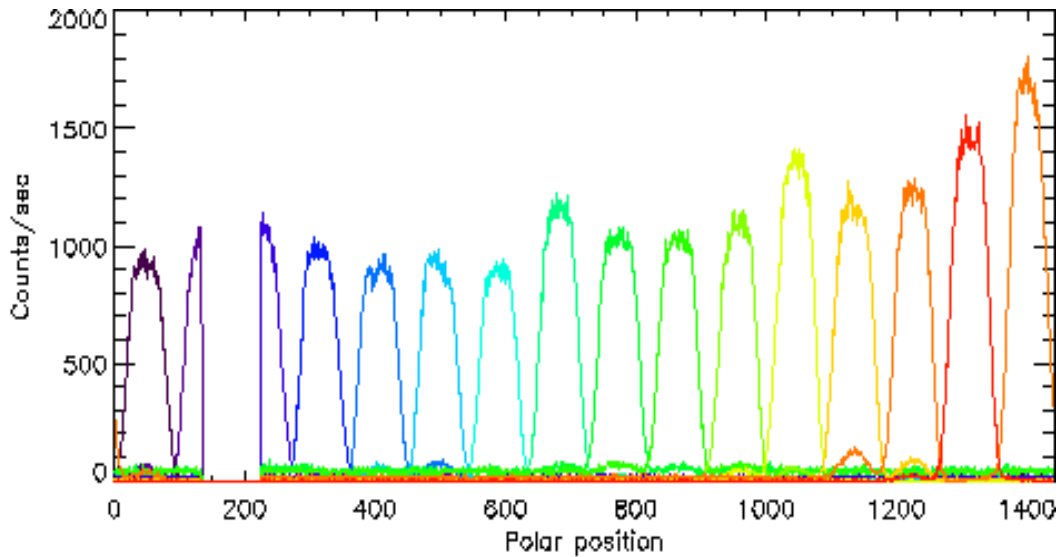


Figure 7: Plot of the analyser response at peak elevation and sweep voltage at fine polar steps in a 100eV beam

7. Energy Table

The Venus Express engineering telemetry (TM) packets include indices representing the deflection reference voltage applied to the ELS. The anode-dependent centre energies are calculated using this TM index. There are two deflection power supplies – the low range supply, which produces a voltage from 0V to 21.8V, and the high range supply which covers 0V to 2777V. For each setting, the TM packet gives the range and the index for the power supply. The index can be between 0 at 4095. If the deflection range is Low, the deflection plate voltage requested is determined by the equation:

$$(3) \quad \text{Low Range Reference Deflection Voltage [volts]} = \text{TM} * (21.8 / 4095)$$

If the deflection range is High, the voltage requested on the deflection plates is determined by the equation:

(4) High Range Reference Deflection Voltage [volts] = TM * (2777.0 / 4095)

To convert these voltages to anode-dependent energies, they are simply multiplied by the k-factors as calculated using the anode-dependent relationship, Equation (1), given in Section 4.

Table 4 shows the centre energy values, for each anode, for the 127 energy steps most commonly used in the standard 4s resolution measurements. It also gives the TM index, and which power supply is being used. Table 5 shows the centre energy values for the 31 energy steps used in the 1s resolution measurements.

Table 4: The anode-dependent 4s energy table using the k-factors from Table 1. Energies in eV.

Power Supply	TM Index	Anode/ Energy	0	1	2	3	4	5	6	7	8	9	10	11	12	13	14	15
Low	16	1	0.89 5892	0.90 3655	0.91 7020	0.93 2436	0.94 7009	0.95 8508	0.96 5360	0.96 6653	0.96 2137	0.95 2219	0.93 7969	0.92 1118	0.90 4053	0.88 9825	0.88 2145	0.88 5383
Low	18	2	1.00 788	1.01 661	1.03 165	1.04 899	1.06 539	1.07 832	1.08 603	1.08 748	1.08 240	1.07 125	1.05 522	1.03 626	1.01 706	1.00 105	0.99 2413	0.99 6056
Low	19	3	1.06 387	1.07 309	1.08 896	1.10 727	1.12 457	1.13 823	1.14 636	1.14 790	1.14 254	1.13 076	1.11 384	1.09 383	1.07 356	1.05 667	1.04 755	1.05 139
Low	21	4	1.17 586	1.18 605	1.20 359	1.22 382	1.24 295	1.25 804	1.26 703	1.26 873	1.26 280	1.24 979	1.23 108	1.20 897	1.18 657	1.16 790	1.15 782	1.16 207
Low	23	5	1.28 784	1.29 900	1.31 822	1.34 038	1.36 133	1.37 786	1.38 770	1.38 956	1.38 307	1.36 881	1.34 833	1.32 411	1.29 958	1.27 912	1.26 808	1.27 274
Low	25	6	1.39 983	1.41 196	1.43 284	1.45 693	1.47 970	1.49 767	1.50 837	1.51 040	1.50 334	1.48 784	1.46 558	1.43 925	1.41 258	1.39 035	1.37 835	1.38 341
Low	27	7	1.51 182	1.52 492	1.54 747	1.57 349	1.59 808	1.61 748	1.62 904	1.63 123	1.62 361	1.60 687	1.58 282	1.55 439	1.52 559	1.50 158	1.48 862	1.49 408
Low	29	8	1.62 380	1.63 787	1.66 210	1.69 004	1.71 645	1.73 730	1.74 971	1.75 206	1.74 387	1.72 590	1.70 007	1.66 953	1.63 860	1.61 281	1.59 889	1.60 476
Low	32	9	1.79 178	1.80 731	1.83 404	1.86 487	1.89 402	1.91 702	1.93 072	1.93 331	1.92 427	1.90 444	1.87 594	1.84 224	1.80 811	1.77 965	1.76 429	1.77 077
Low	35	10	1.95 976	1.97 674	2.00 598	2.03 970	2.07 158	2.09 674	2.11 172	2.11 455	2.10 467	2.08 298	2.05 181	2.01 494	1.97 762	1.94 649	1.92 969	1.93 678
Low	38	11	2.12 774	2.14 618	2.17 792	2.21 454	2.24 915	2.27 646	2.29 273	2.29 580	2.28 507	2.26 152	2.22 768	2.18 765	2.14 713	2.11 333	2.09 509	2.10 279
Low	41	12	2.29 572	2.31 561	2.34 986	2.38 937	2.42 671	2.45 618	2.47 373	2.47 705	2.47 548	2.46 006	2.40 355	2.36 036	2.31 664	2.28 018	2.26 050	2.26 879
Low	45	13	2.51 970	2.54 153	2.57 912	2.62 248	2.66 346	2.69 580	2.71 507	2.71 871	2.70 601	2.67 812	2.63 804	2.59 064	2.54 265	2.50 263	2.48 103	2.49 014
Low	49	14	2.74 367	2.76 744	2.80 837	2.85 559	2.90 022	2.93 543	2.95 641	2.96 038	2.94 654	2.91 617	2.87 253	2.82 092	2.76 866	2.72 509	2.70 157	2.71 149
Low	53	15	2.96 764	2.99 336	3.03 763	3.08 869	3.13 697	3.17 506	3.19 775	3.20 204	3.18 708	3.15 423	3.10 702	3.05 120	2.99 467	2.94 755	2.92 211	2.93 283
Low	57	16	3.19 162	3.21 927	3.26 688	3.32 180	3.37 372	3.41 468	3.43 909	3.44 370	3.42 761	3.39 228	3.34 152	3.28 148	3.22 069	3.17 000	3.14 264	3.15 418
Low	62	17	3.47 158	3.50 166	3.55 345	3.61 319	3.66 966	3.71 422	3.74 077	3.74 578	3.72 828	3.68 985	3.63 463	3.56 933	3.50 320	3.44 807	3.41 831	3.43 086
Low	68	18	3.80 754	3.84 053	3.89 734	3.96 285	4.02 479	4.07 366	4.10 278	4.10 828	4.08 908	4.04 693	3.98 637	3.91 475	3.84 222	3.78 176	3.74 912	3.76 288
Low	74	19	4.14 350	4.17 940	4.24 122	4.31 252	4.37 992	4.43 310	4.46 479	4.47 077	4.47 988	4.40 401	4.33 811	4.26 017	4.18 124	4.11 544	4.07 992	4.09 490
Low	80	20	4.47 946	4.51 827	4.58 510	4.66 218	4.73 505	4.79 254	4.82 680	4.83 327	4.81 068	4.76 110	4.68 985	4.60 559	4.52 026	4.44 913	4.41 073	4.42 692
Low	87	21	4.87 141	4.91 362	4.98 630	5.07 012	5.14 936	5.21 189	5.24 914	5.25 618	5.23 162	5.17 769	5.10 021	5.00 858	4.91 579	4.83 842	4.79 666	4.81 427
Low	95	22	5.31 936	5.36 545	5.44 481	5.53 634	5.62 287	5.69 114	5.73 182	5.73 950	5.71 269	5.65 380	5.56 919	5.46 914	5.36 781	5.28 334	5.23 774	5.25 696
Low	103	23	5.76 731	5.81 728	5.90 332	6.00 256	6.09 637	6.17 039	6.21 450	6.22 283	6.19 375	6.12 991	6.03 818	5.92 969	5.81 984	5.72 825	5.67 881	5.69 965
Low	112	24	6.27 124	6.32 558	6.41 914	6.52 705	6.62 906	6.70 955	6.75 752	6.76 657	6.73 496	6.66 553	6.56 579	6.44 782	6.32 837	6.22 878	6.17 501	6.19 768
Low	121	25	6.77 518	6.83 389	6.93 496	7.05 155	7.16 176	7.24 872	7.30 053	7.31 031	7.27 616	7.20 116	7.09 339	6.96 595	6.83 690	6.72 930	6.67 122	6.69 571
Low	132	26	7.39	7.45	7.56	7.69	7.81	7.90	7.96	7.97	7.93	7.85	7.73	7.59	7.45	7.34	7.27	7.30

Table 5: The anode-dependent 1s energy table using the k-factors from Table 1. Energies in eV.

Power Supply	TM Index	Anode/Energy	0	1	2	3	4	5	6	7	8	9	10	11	12	13	14	15
Low	151	1	8.45 498	8.52 824	8.65 438	8.79 986	8.93 740	9.04 592	9.11 058	9.12 279	9.08 016	8.98 657	8.85 209	8.69 305	8.53 200	8.39 773	8.32 524	8.35 580
Low	168	2	9.40 687	9.48 837	9.62 871	9.79 058	9.94 360	10.0 643	10.1 363	10.1 499	10.1 024	9.99 830	9.84 868	9.67 174	9.49 255	9.34 316	9.26 252	9.29 653
Low	188	3	10.5 267	10.6 179	10.7 750	10.9 561	11.1 274	11.2 625	11.3 430	11.3 582	11.3 051	11.1 886	11.0 211	10.8 231	10.6 226	10.4 554	10.3 652	10.4 033
Low	209	4	11.7 026	11.8 040	11.9 786	12.1 799	12.3 703	12.5 205	12.6 100	12.6 269	12.5 679	12.4 384	12.2 522	12.0 321	11.8 092	11.6 233	11.5 230	11.5 653
Low	234	5	13.1 024	13.2 159	13.4 114	13.6 369	13.8 500	14.0 182	14.1 184	14.1 373	14.0 712	13.9 262	13.7 178	13.4 713	13.2 218	13.0 137	12.9 014	12.9 487
Low	261	6	14.6 142	14.7 409	14.9 589	15.2 104	15.4 481	15.6 357	15.7 474	15.7 685	15.6 949	15.5 331	15.3 006	15.0 257	14.7 474	14.5 153	14.3 900	14.4 428
Low	291	7	16.2 940	16.4 352	16.6 783	16.9 587	17.2 237	17.4 329	17.5 575	17.5 810	17.4 989	17.3 185	17.0 593	16.7 528	16.4 425	16.1 837	16.0 440	16.1 029
Low	325	8	18.1 978	18.3 555	18.6 270	18.9 401	19.2 361	19.4 697	19.6 089	19.6 351	19.5 434	19.3 420	19.0 525	18.7 102	18.3 636	18.0 746	17.9 186	17.9 843
Low	363	9	20.3 256	20.5 017	20.8 049	21.1 546	21.4 853	21.7 461	21.9 016	21.9 309	21.8 285	21.6 035	21.2 802	20.8 979	20.5 107	20.1 879	20.0 137	20.0 871
Low	406	10	22.7 333	22.9 302	23.2 694	23.6 606	24.0 304	24.3 221	24.4 960	24.5 288	24.4 142	24.1 626	23.8 010	23.3 734	22.9 403	22.5 793	22.3 844	22.4 666
Low	453	11	25.3 649	25.5 847	25.9 631	26.3 996	26.8 122	27.1 378	27.3 317	27.3 684	27.2 405	26.9 597	26.5 563	26.0 791	25.5 960	25.1 932	24.9 757	25.0 674
Low	505	12	28.2 766	28.5 216	28.9 434	29.4 300	29.8 900	30.2 529	30.4 692	30.5 100	30.3 674	30.0 544	29.6 047	29.0 728	28.5 342	28.0 851	27.8 427	27.9 449
Low	564	13	31.5 802	31.8 538	32.3 250	32.8 684	33.3 821	33.7 874	34.0 289	34.0 745	33.9 153	33.5 657	33.0 634	32.4 694	31.8 679	31.3 663	31.0 956	31.2 098
Low	630	14	35.2 758	35.5 814	36.1 077	36.7 147	37.2 885	37.7 412	38.0 110	38.0 620	37.8 841	37.4 936	36.9 325	36.2 690	35.5 971	35.0 369	34.7 345	34.8 620
Low	703	15	39.3 633	39.7 043	40.2 916	40.9 689	41.6 092	42.1 144	42.4 155	42.4 723	42.2 739	41.8 381	41.2 120	40.4 716	39.7 218	39.0 967	38.7 593	38.9 015
Low	785	16	43.9 547	44.3 356	44.9 913	45.7 476	46.4 626	47.0 268	47.3 630	47.4 264	47.2 048	46.7 183	46.0 191	45.1 923	44.3 551	43.6 570	43.2 802	43.4 391
Low	877	17	49.1 061	49.5 316	50.2 642	51.1 091	51.9 080	52.5 382	52.9 138	52.9 847	52.7 371	52.1 935	51.4 125	50.4 888	49.5 534	48.7 735	48.3 526	48.5 301
Low	979	18	54.8 174	55.2 924	56.1 102	57.0 534	57.9 451	58.6 487	59.0 679	59.1 471	58.8 707	58.2 639	57.3 920	56.3 609	55.3 167	54.4 462	53.9 762	54.1 744
Low	1092	19	61.1 446	61.6 744	62.5 866	63.6 388	64.6 334	65.4 182	65.8 858	65.9 741	65.6 658	64.9 890	64.0 164	62.8 663	61.7 016	60.7 306	60.2 064	60.4 274
Low	1220	20	68.3 118	68.9 037	69.9 228	71.0 982	72.2 094	73.0 862	73.6 087	73.7 073	73.3 629	72.6 067	71.5 202	70.2 352	68.9 340	67.8 492	67.2 636	67.5 105
Low	1362	21	76.2 628	76.9 236	78.0 613	79.3 736	80.6 142	81.5 930	82.1 762	82.2 863	81.9 019	81.0 576	79.8 447	78.4 101	76.9 575	75.7 464	75.0 926	75.3 682
Low	1520	22	85.1 097	85.8 472	87.1 169	88.5 814	89.9 659	91.0 582	91.7 092	91.8 320	91.4 030	90.4 608	89.1 071	87.5 062	85.8 850	84.5 334	83.8 038	84.1 114
Low	1697	23	95.0 206	95.8 439	97.2 615	98.8 965	100. 442	101. 662	102. 388	102. 526	100. 047	99.4 995	97.6 834	95.8 960	94.3 861	93.5 771	93.9 625	93.9 060
Low	1895	24	106. 107	107. 027	108. 610	110. 435	112. 161	113. 523	114. 335	114. 488	113. 953	112. 778	111. 091	109. 095	107. 074	105. 389	104. 479	104. 863
Low	2115	25	118. 426	119. 452	121. 219	123. 256	125. 183	126. 703	127. 608	127. 779	127. 182	125. 871	123. 988	121. 760	119. 504	117. 624	116. 609	117. 037
Low	2361	26	132. 200	133. 346	135. 318	137. 593	139. 743	141. 440	142. 451	142. 642	141. 975	140. 512	138. 409	135. 922	133. 404	131. 305	130. 172	130. 649
Low	2636	27	147. 598	148. 877	151. 079	153. 619	156. 020	157. 914	159. 043	159. 256	158. 512	156. 878	154. 530	151. 754	148. 943	146. 599	145. 333	145. 867
Low	2943	28	164. 788	166. 216	168. 674	171. 510	174. 191	176. 306	177. 566	177. 804	176. 973	175. 149	172. 528	169. 428	166. 428	163. 289	162. 672	162. 855
Low	3286	29	183. 994	185. 588	188. 333	191. 499	194. 492	196. 854	198. 261	198. 526	197. 599	195. 652	192. 635	189. 175	185. 709	182. 062	181. 749	181. 836
Low	3668	30	205. 383	207. 163	210. 227	213. 761	217. 102	219. 738	221. 309	221. 605	220. 570	218. 296	215. 030	211. 166	207. 254	203. 992	202. 232	202. 974
Low	4095	31	229. 292	231. 279	234. 700	238. 645	242. 375	245. 318	247. 072	247. 403	246. 247	243. 709	240. 062	235. 749	231. 381	227. 740	225. 774	226. 603

8. Geometric Factors

The geometric factor, [GF], in units of $\text{cm}^2 \text{ sr eV/eV}$, is given by

$$(5) \quad [\text{GF}] = (\text{e} \Delta E \Delta \theta \Delta \phi) / (\text{E} * \text{T}_C) \sum_l \sum_m \sum_n N_{lmn} / I_{lmn}$$

where: ΔE = Spacing between calibration points in energy,

$\Delta \theta$ = Elevation spacing,

$\Delta \phi$ = Azimuth spacing,

E = Peak transmitted energy,

T_C =Accumulation time,

I =Beam current in ELS aperture per unit area,

N =ELS counts.

The geometric factors measured in the laboratory by Dhiren Kataria are displayed in Table 6. Note that [GF] incorporates both the purely geometric response of the instrument as well as the detector response.

Table 6: Laboratory measured geometric factors ($\text{cm}^2 \text{ sr eV/eV}$)

Energy(eV) Anode	29.9200	50.3000	70.2000	100.400	199.990	970.000	3021.00	5994.00	9990.00	11997.0
0	2.07540e-006	3.37581e-006	4.73706e-006	6.46449e-006	8.85756e-006	1.08817e-005	8.04262e-006	6.94579e-006	7.42996e-006	5.75665e-006
1	4.57159e-006	5.38168e-006	6.13679e-006	7.10438e-006	9.63588e-006	1.07470e-005	8.32344e-006	7.52185e-006	8.14427e-006	6.11427e-006
2	5.28905e-006	5.95252e-006	6.63087e-006	7.39277e-006	9.47093e-006	9.99465e-006	8.43561e-006	7.54510e-006	7.78974e-006	5.80410e-006
3	4.10182e-006	5.07612e-006	5.80111e-006	6.61061e-006	8.70769e-006	9.52572e-006	8.44829e-006	7.37566e-006	7.42463e-006	5.69616e-006
4	2.75657e-006	4.23158e-006	5.19947e-006	6.14290e-006	8.25067e-006	9.26740e-006	8.10313e-006	6.92202e-006	7.06366e-006	5.36508e-006
5	3.12045e-006	4.36811e-006	5.26247e-006	6.23110e-006	8.07105e-006	8.73019e-006	7.78427e-006	6.40499e-006	6.59983e-006	4.99699e-006
6	3.43856e-006	4.15704e-006	4.80389e-006	5.51189e-006	7.23690e-006	8.07841e-006	7.01710e-006	5.74396e-006	5.92093e-006	4.49043e-006
7	4.06785e-006	4.84366e-006	5.58990e-006	6.32900e-006	8.70944e-006	9.17226e-006	7.42745e-006	5.87616e-006	6.33978e-006	4.69977e-006
8	4.72466e-006	5.15194e-006	5.69955e-006	6.96500e-006	8.51592e-006	9.72213e-006	8.29093e-006	6.61914e-006	7.63213e-006	5.41397e-006
9	4.02959e-006	4.66755e-006	5.74074e-006	7.58045e-006	9.39149e-006	1.06782e-005	9.33263e-006	6.99206e-006	8.69915e-006	5.86279e-006
10	3.20888e-006	4.50439e-006	5.59275e-006	6.49422e-006	8.33294e-006	9.62592e-006	8.62126e-006	6.89954e-006	7.48176e-006	5.68084e-006
11	4.42217e-006	5.77331e-006	6.97938e-006	8.04752e-006	1.03845e-005	1.12857e-005	9.49013e-006	6.46349e-006	8.06194e-006	6.10723e-006
12	3.76111e-006	5.24365e-006	6.59177e-006	8.00591e-006	1.04415e-005	1.29351e-005	1.00476e-005	9.05845e-006	9.09767e-006	7.05230e-006
13	4.43609e-006	5.74996e-006	7.16811e-006	8.55046e-006	1.14662e-005	1.42535e-005	1.07045e-005	9.34059e-006	9.74682e-006	7.63039e-006
14	5.90117e-006	6.89419e-006	8.37360e-006	9.65106e-006	1.17197e-005	1.44310e-005	1.06524e-005	8.89006e-006	9.61936e-006	7.42696e-006
15	6.32660e-006	7.43104e-006	9.01837e-006	1.05006e-005	1.37654e-005	1.49384e-005	1.04071e-005	8.82440e-006	9.39500e-006	7.23438e-006

To find the geometric factor for each of the energies in Table 4, we need to extrapolate from the values in Table 6. The data measured between 199.99 and 5994.00eV in Table 4 are the

most reliable, therefore we only use those in the extrapolation. The best fit is found if we perform the interpolation in log-log space.

9. Calculating Raw Data from Telemetry

Due to the compression of the science values, the way in which the science data decodes is a bit complicated. First we need to figure out the science data structure and we need to decompress the data.

There are five quantities which are important when reconstructing the science data matrix. The first important quantity is the Rice Compression bit. When the Rice compression bit is set, the science data is Rice compressed. In order to be decoded, the science values within the ELS science data packet must be Rice decoded. This must happen before any decoding of the packet. Use the IRF Rice decode software to Rice decode the science data within the packet. If the Rice compression bit is not set, then the science data is not Rice compressed. Rice coding is a lossless data compression scheme to conserve the number of bits in the Venus Express mass memory.

The second important information is the sector mask. The sector mask tells you which ELS anodes are returning data within the packet. The data order is from anode 0 to anode 15 with each bit of the sensor mask representing the presence of anode data for that anode. The number of bits that are set in the sector mask tells you how many and which anodes have sweeps within the packet.

The third important information is the Log compression bit. This tells you whether the words within the packet are 8-bit or 16-bit. 16-bit words are not log compressed and the log compression bit is set to 0. 8-bit words are log compressed and the log compression bit is set. The 8-bit output value is split in a 4-bit exponent (e) and a 4-bit mantissa (m) according to the formula:

For $e < 2$, $\text{counts} = m$ (for $\text{counts} \leq 32$, the output value is the same as the input value)

For $e \geq 2$, $\text{counts} = (m+16) * 2^{(e-1)}$

The compression of telemetry to 8-bits is a lossy process.

The fourth important information is the energy compression. This tells you how many energy steps are in the sweep. If the value of the energy compression is 0, there are 128 energy steps in the sweep. If the value of the energy compression is 1, there are 64 energy steps in the sweep and each science value represents the sum of two energy step values. If the value of the energy compression is 2, there are 32 energy steps in the sweep and each science value represents the sum of four energy step values. Energy compression occurs between successive energy steps obtained from the deflection values decoded from the ELS engineering data packet. Science values for each energy step are adjusted by dividing the science value by the number of energy steps included within a single science measurement.

The fifth important information is the time compression. This tells you how many sweeps are added together, forming each data value. This information is not relevant to decoding the science data, only in determining the actual value of the science data. The science values are adjusted by dividing the science value by the number of sweeps included in the sum representing a single science measurement. For example, if the time compression is a 3, representing 8 sweeps, divide all of the science values by 8. The Accumulation time for each

energy step is now 28125e-6 sec and there is a latency between accumulations of 3125e-6 sec.

The index indicating time compression was to be an indicator of the number of energy sweeps included with in the sum. However, the Main Unit software does not include the science sweep within the sum if during that accumulation period of the sweeps, the Main Unit outputs an ELS engineering packet. However, it still reports the time compression as if it added the sweep. Thus, unless there is an ELS engineering packet output during the accumulation cycle, the time compression decodes as follows: TM value 0 = 1 spectra in sum, TM value 1 = 2 spectra in sum, TM value 2 = 4 spectra in sum, TM value 3 = 8 spectra in sum, TM value 4 = 16 spectra in sum. When the Main Unit outputs an engineering packet, it discards the science data for the same time period. Thus, the time compression decodes as follows: TM value 0 = 1 spectra in sum, TM value 1 = 1 spectra in sum, TM value 2 = 3 spectra in sum, TM value 3 = 7 spectra in sum, TM value 4 = 15 spectra in sum.

To convert the 16-bit science data value to absolute units, you divide each science value by the number of summed energy step values and divide by the number of sweeps included within the measurement. Expand out the science values to each of the energy steps represented in the ELS engineering data packet (for example, if a 64 step sweep, steps 0 and 1 get the same value, 2 and 3 are the same, etc.). This gives you the number of counts within an ELS accumulation for each of the 128 energy step values.

Now, throw out the last step and any steps which include the last step (for example, in a 64 step sweep, then steps 126 and 127 should be discarded). Since the last step is the flyback step, the science data is not valid and should not be included in the spectrum.

10. Data Calibration

The raw data from the telemetry is in units of counts/accumulation. The accumulation time for the Aspera-3 and 4 ELS is 3.6/128 s. So to convert to counts/second we divide the raw data by the accumulation time:

$$(6) \quad \text{Counts/sec} = \text{raw}/\text{accutime}$$

The differential energy flux (DEF), differential number flux (DNF) and the phase space density (PSD) are all dependent on the geometric factor (GF) and the energy level (en), and thus on the anode (an).

$$(7) \quad \text{DEF(an,en)} [\text{cm}^{-2} \text{ sr}^{-1} \text{ s}^{-1}] = \text{raw}/(\text{GF(an,en}) \times \text{accutime} \times A_A)$$

$$(8) \quad \text{DNF(an,en)} [\text{cm}^{-2} \text{ sr}^{-1} \text{ s}^{-1} \text{ J}^{-1}] = \text{DEF}/(\text{earray(an,en}) \times E)$$

$$(9) \quad \text{PSD(an,en)} [\text{cm}^{-6} \text{ s}^3] = (\text{raw} \times m_e^2)/(\text{GF(an,en}) \times \text{accutime} \times 2 \times (\text{earray(an,en}) \times E)^2 \times A_A)$$

In the above equations, earray is the array that contains all the data in Table 4 or 5, E is the conversion from eV to Joules = 1.602×10^{-19} J, m_e is the mass of an electron = 9.11×10^{-31} kg, and A_A is the active anode area ratio (the proportion of the anode area that actually measures counts) = 0.87.

11. MCP voltage response

This set of tests determined the operational regime of the microchannel plate detector. Tests were carried out with the beam incident on anode 10 and the MCP voltage was raised from 1800V to 2880V. The results for the different energies, normalised to the voltage at 2,580V are shown in Figure 8.

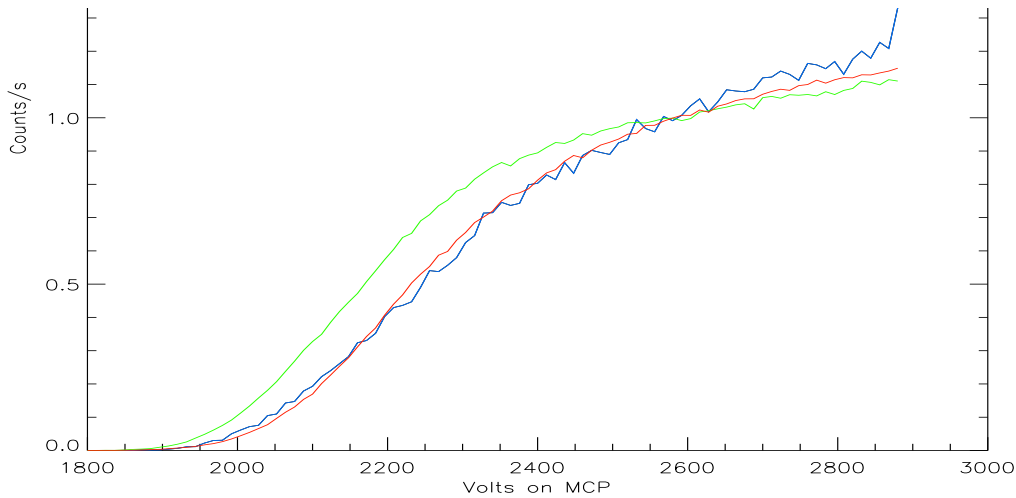


Figure 8: MCP voltage versus normalised counts at 3 energies (30eV: blue, 300eV: green & 10keV: red)

12. UV response

The response of the instrument to UV light has been studied by irradiation of a Krypton UV lamp on the entrance aperture (Alsop et al, 1998). Figure 9 shows the energy angle response of the 16 anodes to UV with the lamp facing Anode 1. As can be seen, most of the counts are observed at very low energies and are primarily due to low energy secondary electrons emitted by the incident light and eventually striking the MCP.

13. Anode selection

Anodes 5-12 have unobstructed views. Anodes 11 and 12 provide the best views and are the most commonly used in data analysis.

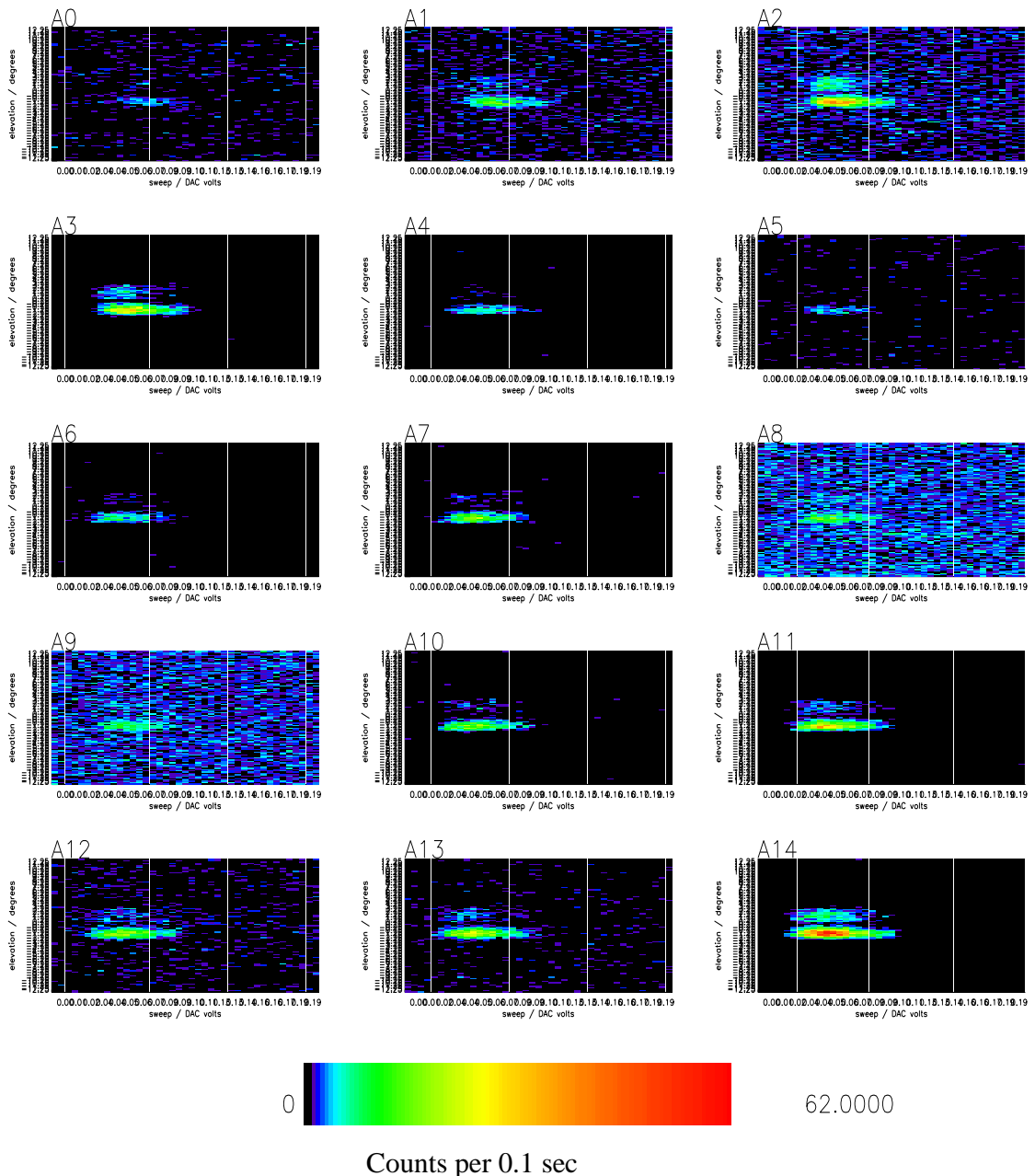


Figure 9: Energy-angle scans for UV response measurement test

14. References

C.Alstop et al, Measurement Techniques In Space Plasmas: Particles, AGU Geophysical Monograph 102, 1998, 269-274

Barabash, S., R. Lundin, H. Andersson, J. Gimholt, M. Holmström, O. Norberg, M. Yamauchi, K. Asamura, A. J. Coates, D. R. Linder, D. O. Kataria, C. C. Curtis, K. C. Hsieh, B. R. Sandel, A. Fedorov, A. Grigoriev, E. Budnik, M. Grande, M. Carter, D. H. Reading, H. Koskinen, E. Kallio, P. Riihela, T. Säles, J. Kozyra, N. Krupp, S. Livi, J. Woch, J. Luhmann, S. McKenna-Lawlor, S. Orsini, R. Cerulli-Irelli, M. Maggi, A. Morbidini, A. Mura, A. Milillo, E. Roelof, D. Williams, J.-A. Sauvaud, J.-J. Thocaven, T. Moreau, D. Winningham, R. Frahm, J. Scherrer, J. Sharber, P. Wurz, and P. Bochsler, ASPERA-3: Analyser of space plasmas and energetic atoms for Mars Express, In *Mars Express – The Scientific Payload*, ESA SP-1240, 121-139, 2004.

A.D.Johnstone, A.J.Coates et al, J.Phys.E:Sci Instrum. **20** (1987), 795-805
Marshall F. J., Hardy D .A. et al, Calibration system for electron detectors in the range from 10 eV to 50 keV, Rev. Sci. Instrum., 57(2), 229-235, 1986.